

# THE INFLOW BOUNDARY CONDITION IN LBGK BLOOD FLOW SIMULATIONS

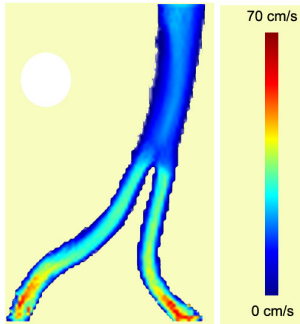
Daniel Leitner<sup>1,2</sup>, Johannes Kropf<sup>1,2</sup>, Siegfried Wassertheurer<sup>1</sup>

<sup>1</sup> Austrian Research Centers GmbH - ARC, Div. Biomedical Engineering, Donau-City-Strae 1, A-1220 Wien

<sup>2</sup> TU Vienna, Institut for Analysis and Scientific Computing Wiedner Hauptstrasse 8-10, A-1040 Vienna

*dleitner@osiris.tuwien.ac.at* (Daniel Leitner)

## Abstract



Recently the Lattice Bhatnagar-Gross-Krook (LBGK) method has been applied to hemodynamical simulations in 3D, giving a powerful tool to investigate blood flow in realistic settings. The geometrical boundary conditions which describe the artery wall can be easily obtained from tomographic images. The choice of reasonable boundary conditions at the in- and outlets is more demanding. To a certain degree the development of self-consistent boundary conditions is as important as the description of the model itself. In LBGK blood flow simulations inflow boundary conditions are of great importance, because pressure boundary conditions must be handled extremely carefully due to the quasi-incompressibility of the method. The problem with these boundary conditions is that the exact velocity profiles at

the in- and outlets are not known beforehand and therefore must be guessed in a realistic way. Different choices of inflow velocity profiles can be made and their influence on the simulation can be analyzed. As an example flow through the abdominal aorta is simulated with time dependent inflow with different velocity profiles. The resulting flow fields, pressure fields and shear stress at the vessel walls are compared and the influence of the different inflows to the overall simulation can be observed.

**Keywords:** Boundary conditions, Lattice Boltzmann Method, LBGK, Hemodynamcis, CFD

## Presenting Author's Biography

Daniel Leitner graduated in mathematics at the Technical University of Vienna. Currently he is working on his doctoral thesis about mesoscopic simulation of blood flow at the Austrian Research Centers. His research interests are numerical modeling, fluid dynamics in general, especially lattice Boltzmann methods and its application to biofluids.



## 1 Introduction

In the western industrial countries cardiovascular diseases are the most frequent cause of death. Therefore a lot of research is done to get a better understanding of the cardiovascular system. Of special interest is the simulation of blood flow in three spatial dimensions using vessel geometries that are obtained from magnetic resonance angiography. This enables an investigation of pressure and flow profiles and shear stress at the vessel wall. The appearing shear stress is important for the risk estimation of arteriosclerosis [1].

In this work a LBGK is used to simulate the blood flow in three spatial dimensions and to solve the incompressible Navier-Stokes equations with the LBGK method [2]. The LBGK method as a hemodynamical solver on tomographic data has been presented in [3]. For the treatment of elasticity of the vessel walls boundary conditions where proposed by [4] where the vessel wall is represented as a surface. When the vessel walls are represented as voxels, a simpler approach has been proposed in [5], which does not need a parameterized representation of the vessel wall.

Blood flow simulation in 3D is mostly restricted to a region of interest, where geometrical data are obtained from tomographic images. The in- and outflow flow profiles are not known and must be chosen in a realistic way. One possibility is to obtain the flow from one-dimensional simulation of the cardiovascular system, see figure 1. There are different ways how to generate a three dimensional flow profile out of a one dimensional parameter like velocity of flow. Different approaches will be compared and the influence of the inflow patterns on the results of the simulation will be discussed.

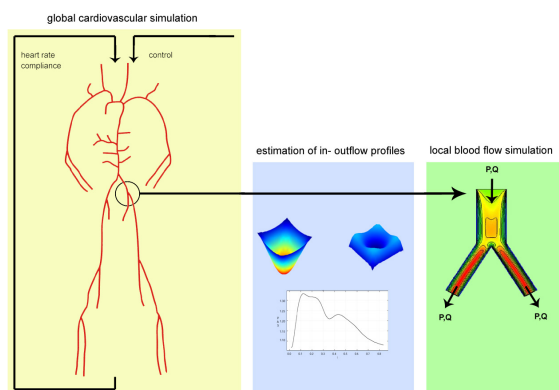


Fig. 1 From a one dimensional model boundary conditions for the more detailed three dimensional model are obtained

## 2 The LBGK D3Q15 method

For simulating the flow field we use the LBGK D3Q15 model. A detailed description can be found in [6] and [2]. The LBGK method has proved to be capable of dealing with pulsative flow within the range of Reynolds and Womersley number existing in large arteries. The LBGK method has been successfully applied to the cardiovascular domain by A.M.M Artoli in [7] and [3]. In the following a short overview of the method shall be given.

LBGK Models are based on a statistical description of a fluid in terms of the Boltzmann equation. Thus it is a bottom up approach in developing a numerical scheme for solving the Navier-Stokes equations. Starting point is the Boltzmann equation with the BGK approximation of the collision integral with single relaxation time is given by

$$\frac{\partial f}{\partial t} + \xi \cdot \nabla f = -\frac{1}{\lambda}(f - f^{eq}) \quad (1)$$

where  $f(\mathbf{x}, \mathbf{v}, t)$  is the probability distribution depending on the spatial coordinate  $\mathbf{x}$ , the velocity  $\mathbf{v}$  and the time  $t$ . The value  $f^{eq}$  is the Maxwell distribution function and  $\xi$  is the macroscopic velocity.

When the Boltzmann is discretised in the spatial domain, in phase space and in time it yields

$$f_i(x + c \cdot \mathbf{c}_i \Delta t, t + \Delta t) - f_i(\mathbf{x}, t) = -\frac{1}{\lambda}(f_i(\mathbf{x}, t) - f_i^{eq}(\mathbf{x}, t)) \quad (2)$$

where  $c = \Delta x / \Delta t$ ,  $\Delta x$  is the lattice grid spacing and  $\Delta t$  the time step. The speed  $c$  couples the spatial and temporal resolution and therefore ensures Lagrangian behavior.

The particle distribution functions  $f_i$  evolve on a regular grid and represent particle densities traveling on the links  $\mathbf{c}_i$ , see figure 2. Thus

$$f_i(\mathbf{x}, t) = f(\mathbf{x}, \mathbf{v}, t) \quad (3)$$

refers to the particle distribution on the lattice node  $\mathbf{x}$  at the time  $t$  with the velocity  $\mathbf{c}_i$ .

The equilibrium density distribution  $f^{eq}(\mathbf{x}, t)$  depends solely on the density  $\rho(\mathbf{x}, t)$  and the velocity  $\mathbf{u}(\mathbf{x}, t)$  of a lattice node  $\mathbf{x}$ . The density  $\rho$  and the velocity  $\mathbf{u}$  are obtained from the density distribution function  $f_i$ . The density is given by

$$\rho(\mathbf{x}, t) = \sum_i f_i(\mathbf{x}, t). \quad (4)$$

Moment and velocity are given by

$$\mathbf{j}(\mathbf{x}, t) = \rho(\mathbf{x}, t) \mathbf{u}(\mathbf{x}, t) = \sum_i \mathbf{c}_i f_i(\mathbf{x}, t) \quad (5)$$

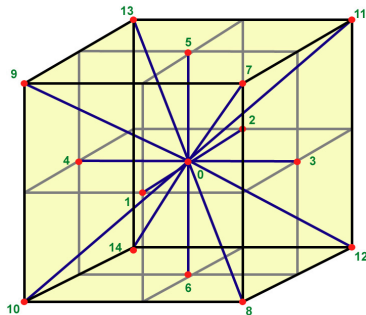


Fig. 2 The velocity directions  $\mathbf{c}_i$  in the D3Q15 LBGK model

The discrete equilibrium distribution function is chosen as

$$f_i^{eq}(\rho, \mathbf{u}) = \omega_i \frac{\rho}{\rho_0} \left( 1 + 3(\mathbf{c}_i \cdot \mathbf{u}) + \frac{9}{2}(\mathbf{c}_i \cdot \mathbf{u})^2 - \frac{3}{2}(\mathbf{u} \cdot \mathbf{u}) \right) \quad (6)$$

with the weight coefficients chosen in the way that the zeros to fourth moments of the equilibrium distribution function equals the Maxwell distribution function.

$$\omega_i = \begin{cases} \frac{2}{9}, & i = 0 \\ \frac{1}{9}, & i = 1, 2, 3, 4, 5, 6 \\ \frac{1}{36}, & i = 7, 8, 9, 10, 11, 12, 13, 14, 15 \end{cases} \quad (7)$$

The mass and momentum equations can be derived from the model via multiscale expansion resulting in

$$\frac{\delta \rho}{\delta t} + \nabla \cdot (\rho \mathbf{u}) = 0 \quad (8)$$

$$\frac{\delta(\rho \mathbf{u})}{\delta t} + \nabla \cdot (\rho \mathbf{u} \mathbf{u}) = -\nabla p + \nu(\nabla^2(\rho \mathbf{u}) + \nabla(\nabla \cdot (\rho \mathbf{u}))) \quad (9)$$

where

$$p = c_s^2 \rho \quad (10)$$

is the pressure,

$$c_s = \frac{c}{\sqrt{3}} \quad (11)$$

is the speed of sound and

$$\nu = \frac{(2\tau - 1)c^2}{6} \Delta t \quad (12)$$

is the kinematic viscosity.

The mass and momentum equations are exactly the same as the compressible Navier- Stokes equation if the density variations are small enough. Thus the compressible Navier- Stokes equation is recovered in the incompressible low Mach number limit.

## 2.1 Implementation

LBGK schemes can be implemented very efficiently because of their explicit and local nature. The pseudo code for LBGK methods can be shortly formulated as

```
while(running) {
  for each node
  {
    calculate kinetic equation
  }
  for each node
  {
    calculate local equilibria
  }
}
```

First the structure of the kinetic equation will be discussed. The kinetic equation 2 can be reformulated as

$$f_i(\mathbf{x} + \mathbf{c}_i, t + 1) - f_i(\mathbf{x}, t) = -\frac{1}{\tau}(f_i(\mathbf{x}, t) - f_i^{eq}) \quad (13)$$

The operator can be split into a collision step and a streaming step in the following way:

$$\begin{aligned} f^*(\mathbf{x}, t) &= \left(1 - \frac{1}{\tau}\right) f_i(\mathbf{x}, t) + \frac{1}{\tau} f_i^{eq} \\ f_i(\mathbf{x} + \mathbf{c}_i, t + 1) &= f^*(\mathbf{x}, t). \end{aligned} \quad (14)$$

This splitting of the operator is called the collide-and-stream update order.

For the knowledge of the equilibrium density distribution  $f_i^{eq}(\rho, \mathbf{j})$  only the node itself, thus no neighborhood, is needed.

The update rules of LBGK methods are simple. Clearly the method works fast and due to its local nature can be easily parallelized. Considering CPUs with multiple cores this benefit of the method is of increasing importance. To adjust the method for multiple threads the set of nodes must be simply distributed on the processors. In each calculated time step the threads must wait for each others two times:

```
while(running)
{
  for each thread
  {
    calculate kinetic equation
    for all nodes
  }

  wait for all threads
  for each thread
  {
    calculate equilibrium values
    for all nodes
  }
  wait for all threads
}
```

### 3 Data acquisition

For geometrical boundary conditions halfway bounce back schemes are used to describe the vessel walls. Tomographic images provide information to determine which nodes are fluid nodes and which are solid no-slip nodes. The images are transformed to a volume consisting of voxels. A binary segmentation of the volume has to be performed mapping every voxel to a corresponding lattice node, see figure 3.

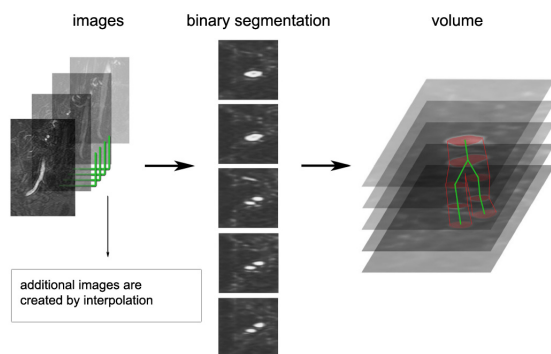


Fig. 3 Binary segmentation of tomographic images

In this way a lattice is constructed that can be used for computer fluid dynamics using the LBGK method. No complicate mesh generation methods are needed like with finite volume or finite element methods. The vessel walls are given in a voxel representation and not as parameterized surfaces.

For the comparison of different in- and outlet boundary conditions a model of abdominal aorta has been created from tomographic images, see figure 9.



Fig. 4 Voxel representation of the abdominal aorta

In the next step realistic boundary conditions for the in- and outlets will be developed.

### 4 Inflow Boundary condition for LBGK

The inflow boundary condition for the LBGK schemes can be implemented easily. In every discrete time step the inflow nodes are reset to the equilibrium population, which corresponds to the desired value of flow speed and density [6].

$$f_{in} = f_{out}^{eq}(\rho_{in}, \mathbf{u}_{in}) \quad (15)$$

In the following considerations  $\rho_{in}$  is set to 1 for simplicity.

The difficult part is to choose the right flow profile. Realistic flow profiles can be obtained from analytical considerations. First laminar flow in cylindrical coordinates is assumed, thus the fluid can only flow parallel to the tube:

$$\begin{aligned} u_r &= 0 \\ u_\phi &= 0 \\ u_z &= u_z(r, t) \end{aligned} \quad (16)$$

When additionally steady flow and constant pressure gradient is assumed this is called a Poiseuille flow and is given by:

$$u_z^P(r) = \frac{(R^2 - r^2)(P_1 - P_2)}{4\mu L}. \quad (17)$$

Another solution is given by Womersley. When laminar flow with pulsating pressure gradient is assumed the so called Womersley flow can be derived analytically:

$$u_z^W(r, t) = \frac{AcR^2}{i\mu\alpha^2} \left( 1 - \frac{J_0(\alpha(r/R)i^{3/2})}{J_0(\alpha i^{3/2})} \right) e^{i\omega t}. \quad (18)$$

For the resulting velocity profiles see figure 5

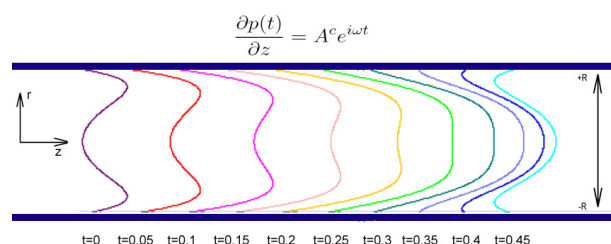


Fig. 5 Velocity profiles of Womersley flow in two dimensions

The two equations are used to create realistic flows at the in- and outlets. Poiseuille flow is used when steady flows are under investigation, while the Womersley flow is used when a dynamic model is calculated.

A problem with this approach is that especially Poiseuille flow is often not fully established in realistic settings [8] because of the effects caused by branching of the vessels. As a result the flow at the inlet has normally a flatter profile than the Poiseuille flow. For this reason the velocity profile which is approximated with

$$u_z^P(r) = (R^N - r^N)c_0 \quad (19)$$

with a constant  $c_0$  for scaling and  $N \geq 2$ , see figure 6. Note that for  $N = 2$  the equation is exactly the Poiseuille equation, for  $N > 2$  a flatter velocity profile is achieved.

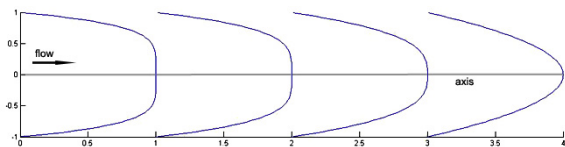


Fig. 6 Velocity profiles at an inlet for different choices of  $N = 5, 4, 3, 2$

The velocity profiles must be scaled to yield the predetermined flow  $q(t)$ . The predetermined flow can be the result of a prediction from a coarser model of the cardiovascular system or can be obtained from measurements. In the following the flow in the abdominal aorta will be simulated with different velocity profiles at the inlet and the influence to the shear stress at the vessel wall will be investigated.

## 5 Shear stress

A nice property of LBGK simulations is the easy calculation of the stress tensor. It can be calculated independent of the velocity gradients with the following simple formula [3]:

$$\sigma_{\alpha\beta} = -\rho c_s^2 \delta_{\alpha\beta} - \left(1 - \frac{1}{2\tau}\right) \sum_{i=0}^{15} f_i^{eq} c_{i\alpha} c_{i\beta}. \quad (20)$$

The stress tensor is used to calculate the von Mises effective stress, which is used to quantify the shear stress at the vessel wall [9]:

$$\sigma_{eff} = \sqrt{\frac{a + 6b}{2}} \quad (21)$$

with

$$a = (\sigma_{xx} - \sigma_{yy})^2 + (\sigma_{yy} - \sigma_{zz})^2 + (\sigma_{zz} - \sigma_{xx})^2 \quad (22)$$

and

$$b = \sigma_{xy}^2 + \sigma_{yz}^2 + \sigma_{zx}^2. \quad (23)$$

The quantity is an invariant of the stress tensor and therefore independent of orientation.

The shear stress is of fundamental importance for blood flow simulation because in local shear stress is related with the clotting process and therefore an important risk factor of arteriosclerosis [1].

## 6 Results

Blood flow is simulated through the abdominal aorta over one cardiac cycle. First the region of interest is defined, see figure 7 and then the volume is cropped to a bounding cube of 4.8 cm \* 8.6 cm \* 2.8 cm. The resulting lattice consists of approximately 26000 fluid nodes and 16000 no-slip boundary nodes, where every node has a size of  $15^{-1}$  cm.

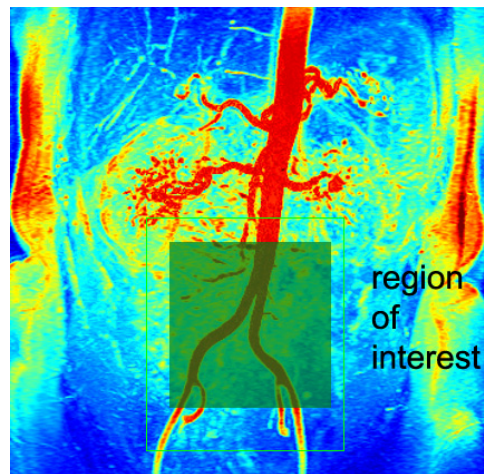


Fig. 7 The definition of the region of interest in a maximum intensity projection of a MRI

The in- and outflow over a cardiac cycle is taken from [8] with a period of 0.7 s. The inflow boundary condition (see equation 15) is used at the in- and outlets.

The inflow velocity profile is chosen in three different ways:

1. The simplest approach is to choose a constant inflow.
2. A fully developed Poiseuille flow.
3. A incompletely developed Poiseuille flow, approximated with equation 19 with  $N = 4$

The inflow is scaled in a way that the time dependent flow  $q(t)$  is achieved, see figure 8.

The flow field is simulated over one cardiac cycle and the effective wall stress is calculated with equation 21.

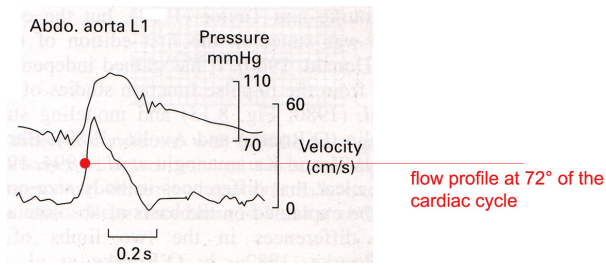


Fig. 8 The inflow  $q(t)$  used for the simulation

The resulting velocity fields at 72 degrees are given in figure 9, where the velocities are plotted with a maximum intensity projection.

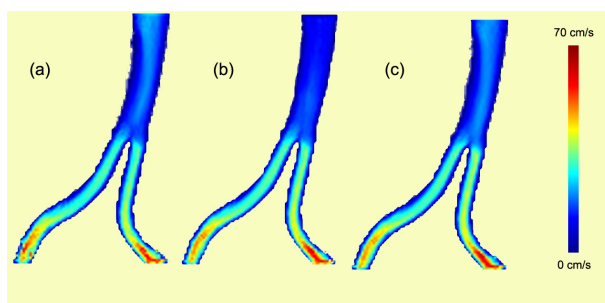


Fig. 9 The resulting velocity fields with fully developed inlet (a), constant inlet (b) and partly developed inlet (c)

The differences at the inlet can be recognized clearly in figure 9, while the flow field at the bifurcation is very similar. The derivation of the wall shear stress in this region is less than one percent which is acceptable, since the error of the tomographic is much bigger (between 1-8% [10]).

## 7 References

- [1] J. Suo, D. E. Ferrara, D. Sorescu, R. E. Gulberg, W. R. Taylor, and D. P. Giddens. Hemodynamic shear stresses in mouse aortas: Implications for atherogenesis. *Arterioscler Thromb Vasc Biol*, 27(2):346–51, 2007.
- [2] D.A. Wolf-Gladrow. *Lattice-Gas Cellular Automata and Lattice Boltzmann Models - An Introduction (Lecture Notes in Mathematics)*. Springer, 2000.
- [3] A.M.M. Artoli, A.G. Hoekstra, and P.M.A. Slood. Mesoscopic simulations of systolic flow in the human abdominal aorta. *Journal of Biomechanics*, 39(5):873–884, 2006.
- [4] H. Fang, Z. Wang, Z. Lin, and M. Liu. Lattice boltzmann method for simulating the viscous flow in large distensible blood vessels. *Phys. Rev. E.*, 2001.
- [5] D. Leitner, S. Wassertheurer, M. Hessinger, and Holzinger A. A lattice boltzmann model for pulsative blood flow in elastic vessels. *Elektronik und Informationstechnik*, (4):152–155, 2006.
- [6] S. Succi. *The Lattice Boltzmann Equation for Fluid Dynamics and Beyond*. Oxford University Press, 2001.
- [7] A.M.M. Artoli, B.D. Kandhai, H.C.J. Hoefsloot, A.G. Hoekstra, and P.M.A. Slood. Lattice bgk simulations of flow in a symmetric bifurcation. *Future Generation Computer Systems*, 20(6):909–916, 2004.
- [8] W.W. Nichols and M.F. O'Rourke. *McDonald's blood flow in arteries*. Arnold, 4 edition, 1998.
- [9] H. Geiringer. Recent results in the theory of plasticity. *Advances in applied mechanics*, 3:200–201, 1935.
- [10] C. A. Taylor, T. J. R. Hughes, and C. K. Zarins. Finite element modeling of three-dimensional pulsatile flow in the abdominal aorta: Relevance to atherosclerosis. *Annals of Biomedical Engineering*, (26):975–987, 1998.